Tight-binding theory for coupled photonic crystal waveguides

F. S.-S Chien
Department of Physics, Tunghai University, Taichung 407, Taiwan

J. B. Tu and W.-F. Hsieh*,†
Department of Photonics and Institute of Electro-Optical Engineering, National Chiao Tung University, Hsinchu 300, Taiwan

S.-C. Cheng*,‡
Department of Physics, Chinese Culture University, Yang-Ming Shan, Taipei 111, Taiwan
(Received 25 May 2006; revised manuscript received 11 October 2006; published 20 March 2007)

The point-defect coupling under the tight-binding approximation is introduced to describe the behavior of dispersion relations of the guided modes in a single photonic crystal waveguide (PCW) and two coupled identical PCWs. The cross-coupling coefficient β of a point defect in one PCW to the nearest-neighboring (NN) defect in the other PCW causes the split of the dispersion curves, whereas the cross-coupling coefficient γ to the next-NN defects causes a sinusoidal modulation to the dispersion curves. Furthermore, the sign of β determines the parities of the fundamental guided modes, which can be either even or odd, and the inequality $|\beta| < |2\gamma|$ is the criterion for the crossing of split dispersion curves. The model developed in this work allows for deriving the coupled-mode equations and the coupling length.

DOI: 10.1103/PhysRevB.75.125113 PACS number(s): 71.15.Ap, 42.70.Qs, 42.79.Gn, 42.82.Et

I. INTRODUCTION

A photonic crystal waveguide (PCW) is formed by introducing a line defect in the perfect photonic crystal (PhC) to create a guided mode or group of guided modes within the band gap.[1] Interest is especially focused on the electromagnetic (EM) wave being guided within the waveguide by the mechanism of band-gap confinement. The PCWs are the most promising elements of PhCs for building large-scale photonic integrated circuits (PICs), because the EM waves can be transmitted,[2] sharply bent,[3] split,[4] and dispersion compensated[5] by means of specific PCW designs.

Waveguide coupling is a fundamental mechanism for designing various optical filters and switches for PICs. Recently, PCW coupling[6] has received much attention, since numerous photonic devices based on this mechanism have been proposed and demonstrated, e.g., filters,[7] switches,[8] and multiplexers and/or demultiplexers.[9,10] Typically, the waveguide coupling is handled by the coupled-mode theory (CMT),[11] which is a straightforward and simple method to give approximate solutions in coupled (perturbed) waveguide systems. The wave behaviors of the coupled system are derived from the eigenmodes of the isolated (unperturbed) waveguides. The concept of CMT has also been applied to interpret the coupling of PCWs.

Two characteristics of the eigenmodes in coupled waveguides are derived from the CMT.[12] First, the fundamental guided mode is of even parity and the second mode is of odd parity. Second, the dispersion curves of eigenmodes of the coupled system should not cross (see Sec. II). Boscolo *et al.*[13] argue that these characteristics exist in coupled PCWs. However, this argument has been challenged, because the dispersion curves derived from the plane-wave expansion (PWE) method reveal that the fundamental guided mode can be odd and the dispersion curves do cross; i.e., the eigenmodes are degenerate and the waveguides are decoupling.[10] An asymptotic model has been employed to demonstrate theoretically that the fundamental mode can be even or odd (depending on the number of partition rows).[14] On the other hand, it is proposed that the change of the "effective parities" of the eigenmodes causes the crossing of the dispersion curves.[15] Evidently, the conventional CMT is inadequate to depict the PCW coupling. A correct waveguide theory in PCWs has to be developed for the characteristics of the eigenmodes.

In this paper, we explore the properties of PCW via the coupling of point defects under the tight-binding approximation,[16] which assumes that the field distribution (or wave function) of an individual point defect is strongly localized around this point defect. The dispersive behavior of a single PCW can be described by the coupling with the neighboring point-defect modes. We further consider the point-defect coupling between two identical PCWs to describe the PCW coupling. The parity of eigenmodes and the crossing of dispersion curves of coupled PCWs depend on the signs and values of the point-defect coupling coefficients across the PCWs. The coupled-mode equations and coupling length are derived based on the point-defect coupling.

II. INSUFFICIENCY OF COUPLED MODE THEORY

Let two conventional waveguides be identical and denoted as I and II. Since the isolated eigenmode is independent of the propagating distance, say, along y, the waveguides are coupled uniformly. The coupled mode equations derived from CMT are expressed as

$$\frac{dU(y)}{dy} = -iCV(y), \quad \frac{dV(y)}{dy} = -iCU(y), \tag{1}$$

and

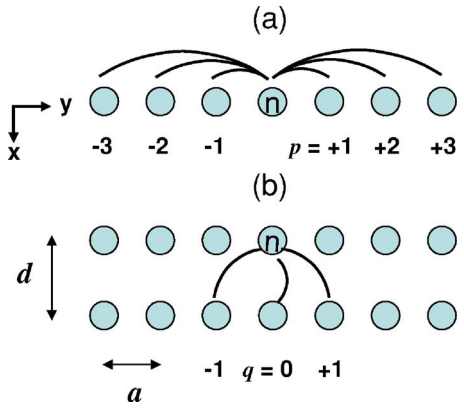

FIG. 1. (Color online) (a) Point-defect coupling to the pth neighboring defect in an isolated PCW and (b) cross coupling to the qth neighboring point defects in the other PCW. The circles represent the defects in a 2D perfect PhC.

$$C = \frac{1}{2}\frac{k_0^2}{k}\int \Delta\varepsilon(x)a(x)b(x)dx, \tag{2}$$

where $U(y)$ and $V(y)$ are the slowly varying amplitudes of the waveguides I and II, C is the coupling coefficient, $a(x)$ and $b(x)$ are the distribution functions of isolated eigenmodes in the transverse direction x, $\Delta\varepsilon(x)$ is the difference of spatial-dependent dielectric constants of the unperturbed (single waveguide) system and the perturbed (coupled waveguide) system, and k_0 and k are the propagation constants of free space and the isolated PCW, respectively.

Because the perturbed system contains two identical waveguides, its eigenmodes possess even and odd parities. Under the weak coupling approximation, they can be expressed in terms of superpositions of U and V. The dispersion curves split, since the even and odd eigenmodes of the same frequency have propagation constants (k_e and k_o), whose difference is $k_e - k_o$. In this case, the total power launched into one waveguide will be transferred completely to the other if the EM wave propagates a coupling length $l_c = \pi/|k_e - k_o|$, in which $|k_e - k_o|$ equals $2C$. The degeneracy of even and odd modes, i.e., $k_e = k_o$, implies $C=0$. From Eq. (2), $C=0$ appears only if $\Delta\varepsilon(x)=0$, meaning that the waveguides are merged into one waveguide. Therefore, the conventional CMT does not suggest the crossing of dispersion curves, which exists in coupled PCW system.[10]

III. ISOLATED PHOTONIC CRYSTAL WAVEGUIDE: COUPLING BETWEEN CONSECUTIVE POINT DEFECTS

We begin our analysis by considering a periodic sequence of identical coupled defects, as shown schematically in Fig. 1(a). The distance between successive point defects (or primitive cells) is a. Furthermore, we assume that each defect mode is single mode, oscillating at an eigenfrequency ω_0. The EM mode of each defect in isolation is given by $\mathbf{E}(\mathbf{r},t) = u(t)\mathbf{E}_0(\mathbf{r})$, where $\mathbf{E}_0(\mathbf{r})$ and $u(t) = U\exp(-i\omega_0 t)$ represent the spatial and time-varying functions of the defect eigenmode. Here, U is a constant. Evidently, because of proximity, finite coupling should exist between successive defects in a linear PCW. Hence, the dispersion relation of the guided mode results from the coupling of longitudinally shifted point-defect modes; namely, each point defect, say the defect site n, is coupled with other defects at sites $n+p$, where p is an integer. Under the tight-binding approximation, the field vector $\mathbf{E}_n(\mathbf{r})$ at the defect site n is not perturbed much by the presence of the other defects and can be expressed as $\mathbf{E}_n(\mathbf{r}) = \mathbf{E}_0(\mathbf{r} - na\hat{\mathbf{y}})$, where $\hat{\mathbf{y}}$ is the unit direction vector along the line defect. Therefore, the total field is a summation over the field vectors of all defect sites as $\mathbf{E}(\mathbf{r},t) = \Sigma u_n(t)\mathbf{E}_n(\mathbf{r})$, where $u_n(t)$ is the time-varying amplitude of the perturbed field at site n. We derived the coupled equation under the slowly varying amplitude approximation[17] as

$$i\frac{\partial}{\partial t}u_n = (\omega_0 - c_0)u_n - \sum_{p=1} c_p(u_{n+p} + u_{n-p}) \tag{3}$$

to relate u_n with $u_{n\pm p}$ (the amplitude of the $\pm p^{\text{th}}$ neighboring defect site from the defect site n), where c_p is the coupling coefficient between point defects n and $n+p$ [illustrated in Fig. 1(a)] and is written as

$$c_p = \frac{\omega_0 \int \Delta\varepsilon(\mathbf{r})\mathbf{E}_0(\mathbf{r} - na\hat{\mathbf{y}}) \cdot \mathbf{E}_0[\mathbf{r} - (n+p)a\hat{\mathbf{y}}]d^3r}{\int [\mu_0|\mathbf{H}_0(\mathbf{r} - na\hat{\mathbf{y}})|^2 + \varepsilon|\mathbf{E}_0(\mathbf{r} - na\hat{\mathbf{y}})|^2]d^3r}, \tag{4}$$

where $\Delta\varepsilon(\mathbf{r}) = \varepsilon'(\mathbf{r}) - \varepsilon(\mathbf{r})$ is the difference of spatial-dependent dielectric constants of the unperturbed system (single defect) $\varepsilon(\mathbf{r})$ and the perturbed system (coupled defects) $\varepsilon'(\mathbf{r})$, and $p = 0, 1, 2, \ldots$. Thus, c_0 with $p=0$ represents a small shift to the eigenfrequency ω_0 of the isolated point defect due to the dielectric perturbation of the neighboring defects, to which the eigenfield of the isolated point defect extends. Let $u_n(t) = U_0\exp(ikna - i\omega_1 t)$, where k is the propagation constant and U_0 is the constant amplitude. Substituting this into Eq. (3), we obtain the dispersion relation of a PCW as

$$\omega_1(k) = \omega_0 - c_0 - \sum_{p=1} 2c_p\cos(pka). \tag{5}$$

The term $2c_p\cos(pka)$ is attributed to the polarization at site n by the field at $\pm p$th neighboring defects.

Assume the PCW consists of a line defect of reduced rods in a two-dimensional PhC with a square array of circular rods. Let the dielectric constant ε_d of the rod be 12, the radius of the rod $0.2a$, the radius of the defect (reduced rod) $0.1a$, and the dielectric constant of air $\varepsilon_a = 1$. The dispersion curve and the wave function of a single PCW with E polarization (i.e., the electric field is parallel to the dielectric rods) can be calculated using the PWE method, in which the fully vectorial eigenmodes of Maxwell's equations with periodic boundary conditions are computed on a plane-wave basis.[18] The dotted data shown in Fig. 2 are the discrete values of the dispersion calculated using PWE. The resolution is determined by how many plane waves or k's are used in the

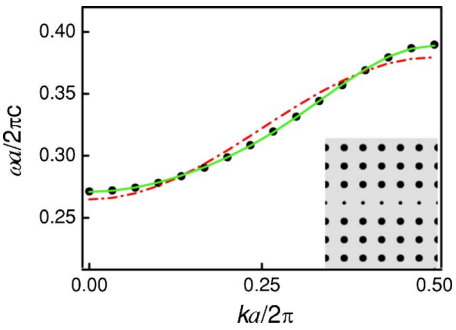

FIG. 2. (Color online) Dispersion curves of a reduced-rod PCW in a square lattice (inset), calculated by PWE (data dots) and fitted with the formula considering the point-defect only coupling to NN defects (dashed line) and coupling up to the third NN defects (solid line).

expansion. Since the eigenfield distribution extends more than the nearest-neighboring (NN) site (Fig. 3), the dispersion does not fit well with the formula

$$\omega_1(k) = \omega_0 - c_0 - 2c_p \cos(pka). \tag{6}$$

This describes the so-called coupled-resonator optical waveguide (CROW),[19,20] in which the defects are not consecutive (i.e., are well separated) and are weakly coupled. The coupling in a CROW is so weak that the wave hops to its NN defects ($p=\pm 1$) due to the overlapping of the evanescent waves; therefore, only the NN defects are involved in the dispersion relation (shown as the dashed curve in Fig. 2). However, the dispersion is well fitted as long as the couplings up to the third NN defects are taken into account (shown as the solid curve in Fig. 2). Therefore, we truncate Eq. (5) as

$$\omega_1(k) = \omega_0 - c_0 - 2c_1 \cos(ka) - 2c_2 \cos(2ka) - 2c_3 \cos(3ka), \tag{7}$$

hereafter to describe a consecutive line-defect PCW.

As the point defects are not well separated, their eigenfields do extend over three lattice constants away in the consecutive line-defect PCW, as shown in Fig. 3 for a reduced-rod PCW in a square lattice and in Fig. 4 in a triangular lattice. Therefore, up to the third NN coupling has to be considered to fit the dispersion curve well. On the other hand, we can directly integrate the overlap integrals of Eq. (4) to obtain the coupling coefficients of Eq. (7). Basically, it should give the same results since the fitting is quite good. Although the change of dielectric constant is a negative step function [$\Delta\varepsilon(r)=\varepsilon_a-\varepsilon_d, <0$ at all defect sites and 0 otherwise], there is no simple way to accurately calculate c_p without the complicated integration using Eq. (4) because the field is not symmetrical and not located at the center of each dielectric rod (see Figs. 3 and 4). Furthermore, because Eq. (7) contains only four coupling coefficients (fitting parameters), several ($\geqslant 5$) discrete k's in the first Brillouin zone are enough, which reduces the computation time for calculating the dispersion curves.

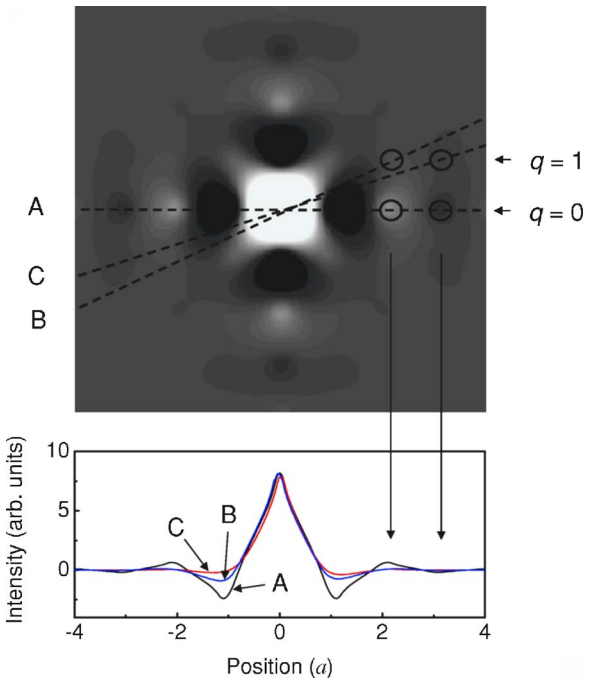

FIG. 3. (Color online) (Upper panel) The electric eigenfield pattern of a reduced-rod defect in a square lattice, where circles indicate the equivalent sites of the NN ($q=0$) and next-NN defects ($q=+1$) when the other PCW is separated by one and two partition rows. (Lower panel) The projected profiles (denoted as A, B, and C) passing through various sites of neighboring defects. The gray scale represents the electric field intensity with white for positive and black for negative.

IV. TWO COUPLED IDENTICAL PHOTONIC CRYSTAL WAVEGUIDES: COUPLING AMONG A NETWORK OF POINT DEFECTS

As presented in the previous section, a single PCW can be regarded as a chain of coupled point defects, and its field distribution is no longer uniform along the propagation direction but involves localization. Similarly, the coupled PCWs can be regarded as a network of coupled point defects, so that the concept of point-defect coupling should be able to describe the behavior of coupled PCWs. In addition to the longitudinal coupling with point defects within the native PCW, the "cross coupling" with the point defects across from the other PCW is involved, as shown in Fig. 1(b). We consider two parallel identical PCWs (denoted as I and II) separated by some rows of partition rods (or by a distance d). Conceivably, the cross coupling with the NN defect ($q=0$) and the next-NN defects ($q=\pm 1$) are dominant and will be taken into account. Let β and γ represent the cross-coupling coefficients of site n with defects $q=0$ and $q=\pm 1$. Note that β and γ have the same form as Eq. (4), while $\mathbf{E}_0[\mathbf{r}-(n+p)a\hat{\mathbf{y}}]$ is replaced by $\mathbf{E}_0[\mathbf{r}-(n+q)a\hat{\mathbf{y}}+d\hat{\mathbf{x}}]$, where d is the distance between two line defects. The couplings with the farther defects ($q\geqslant 2$) are negligible, since the corresponding coefficients are relatively smaller than β and γ (we will show later, in a specific case, that the coupling coefficient with $q=2$ is only 1/7 of γ). The coupled equation of an isolated PCW [Eq. (7)] can be extended for two coupled PCWs, given as

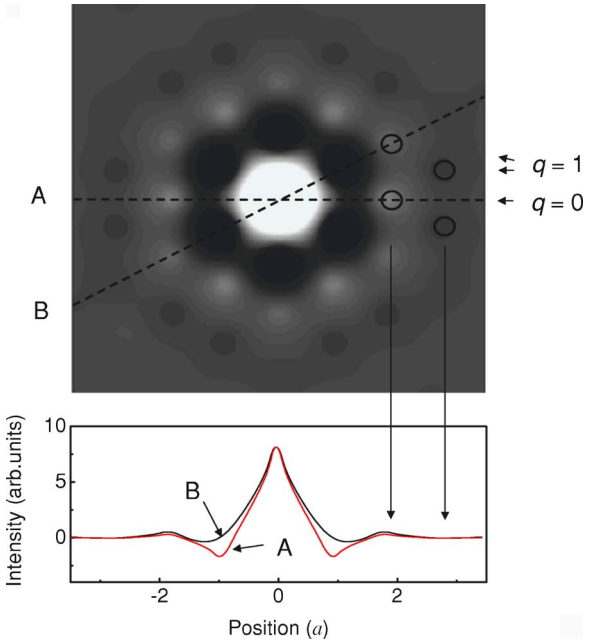

FIG. 4. (Color online) (Upper panel) The electric eigenfield pattern of a single reduced-rod defect in a triangular lattice, where circles indicate the equivalent sites of the NN and next-NN defects when the other PCW is separated by one and two partition rows. (Lower panel) The projected profiles (denoted as A and B) passing through various sites of neighboring defects.

$$i\frac{\partial}{\partial t}u_n = (\omega_0 - c_0)u_n - \sum_{p=1}^{3} c_p(u_{n+p} + u_{n-p}) - \beta v_n - \gamma(v_{n+1} + v_{n-1}), \tag{8}$$

$$i\frac{\partial}{\partial t}v_n = (\omega_0 - c_0)v_n - \sum_{p=1}^{3} c_p(v_{n+p} + v_{n-p}) - \beta u_n - \gamma(u_{n+1} + u_{n-1}), \tag{9}$$

where $u_n(t)$ and $v_n(t)$ represent the amplitudes at specific point defects in PCWs I and II, respectively. Let the solutions be $u_n(t)=U_0\exp(ikna-i\omega_2 t)$ and $v_n(t)=V_0\exp(ikna-i\omega_2 t)$ and be substituted into Eqs. (8) and (9). The characteristic equations of the coupled PCWs are obtained as

$$(\omega_2 - \omega_1)U_0 + [\beta + 2\gamma\cos(ka)]V_0 = 0, \tag{10}$$

$$(\omega_2 - \omega_1)V_0 + [\beta + 2\gamma\cos(ka)]U_0 = 0, \tag{11}$$

where $\omega_1(k)$ is the fitted dispersion relation of the isolated PCW given in Eq. (7). Again, U_0 and V_0 are the constant field amplitudes of PCWs I and II, respectively. Therefore, the dispersion relations of the coupled PCWs can be obtained from the characteristic equations [Eqs.(10) and (11)] as

$$\omega_2(k) = \omega^{\pm}(k) = \omega_1(k) \pm [\beta + 2\gamma\cos(ka)]. \tag{12}$$

The dispersion of the identical (degenerate) PCWs is split into two curves, denoted as $\omega^+(k)$ and $\omega^-(k)$, due to the cross coupling.

Obviously, the cross coupling with the $q=0$ defect leads only to a relative shift of eigenfrequency by $\pm\beta$, and that with neighboring defects $q=1$ and -1 leads to the sinusoidal modulation $[\pm 2\gamma\cos(ka)]$ of the dispersion curves. There is competition between β (the contribution from the $q=0$ defect) and the term $\pm 2\gamma\cos(ka)$ (from $q=\pm 1$ defects). If $|\beta| < |2\gamma|$ (i.e., the total cross-coupling strength of $q=\pm 1$ defects surpasses that of the $q=0$ defect), the intersection of dispersion curves occurs at wave number $k=[\cos^{-1}(-\beta/2\gamma)]/a$, where $\beta+2\gamma\cos(ka)=0$. This implies that the cross couplings with $q=0$ and both ± 1 defects are exactly canceled out. Accordingly, the three curves of ω_1, ω^+, and ω^- are bound to the crossing point ($\omega^{\pm}=\omega$), where the split guided modes are degenerate and the PCWs are decoupled (implying that the presence of the second PCW can be ignored). The inequality $|\beta| < |2\gamma|$ is a necessity for the dispersion crossing that originates from the cross coupling with the $q=\pm 1$ neighboring defects, due to the nonuniform nature along the propagation direction of the mode function of individual PCWs. Such a cross coupling does not exist in conventional waveguides, since the wave functions of conventional waveguides are uniform along the propagation direction. Therefore, the dispersion curves of two identical conventional waveguides can never cross.

Substituting Eq. (12) into Eqs. (10) and (11) we obtain the corresponding eigenvectors for describing the constant amplitudes of the two dispersion relations $\omega^+(k)$ and $\omega^-(k)$ as

$$\begin{pmatrix} U_0^+ \\ V_0^+ \end{pmatrix} = \begin{pmatrix} 1 \\ -1 \end{pmatrix} \quad \text{for } \omega_2(k) = \omega^+(k) \quad \text{and}$$

$$\begin{pmatrix} U_0^- \\ V_0^- \end{pmatrix} = \begin{pmatrix} 1 \\ 1 \end{pmatrix} \quad \text{for } \omega_2(k) = \omega^-(k), \tag{13}$$

respectively. The eigenmode of $\omega^+(k)$ has odd parity, while that of $\omega^-(k)$ has even parity. Thus, ω^+ (ω^-) is the fundamental guided mode, if β is negative (positive). Here, the fundamental guided mode is referred to as the guided mode with lowest frequency at $k=0$. Therefore, the parity of the fundamental guided mode (determined by the sign of β) can be either even or odd, consistent with the asymptotic model.[14]

A. Reduced-rod defects in square lattices

β and γ govern the properties of coupled PCWs, since the system can be regarded as a network of coupled point defects. According to Eq. (4), β and γ are proportioned to the autocorrelation of the eigenfunction with origins shifted relative to $d\hat{\mathbf{x}}$ and $d\hat{\mathbf{x}}+a\hat{\mathbf{y}}$ [or denoted as $S(d\hat{\mathbf{x}})$ and $S(d\hat{\mathbf{x}}+a\hat{\mathbf{y}})$], calculated at the defect sites and then multiplied by the negative step function $\Delta\varepsilon$, where again $\hat{\mathbf{x}}$ and $\hat{\mathbf{y}}$ are the unit vectors along the x and y directions. Therefore, the eigenfield of a single defect can deliver much information on coupled PCWs. For the case of a single reduced-rod defect in a square lattice, the eigenfield of E polarization derived by PWE is localized at the defect center and decreases rapidly with radial distance (see the upper panel of Fig 3). The radial field profiles along various directions are shown in the lower panel of Fig. 3. The peaks and valleys alternately appear

TABLE I. Crossing vs $\beta/2\gamma$ and parity of fundamental mode vs sign of β for coupled PCWs with reduced-rod and void-rod defects in square and triangular lattices.

Defect rods		Reduced				Void	
Lattice		Square		Triangular		Square	
Partition rows		1	2	1	2	1	2
Crossing by PWE[a]		No	No	Yes	Yes	Yes	No
$\lvert\beta/2\gamma\rvert$	Estimated with Eq. (4)	4.6	2	0.9	N.A.	1.2	0.96
	Fitted with Eq. (12)	5.2	1.4	0.75	0.67	0.69	1.15
Parity of fundamental mode by PWE[a]		Odd	Even	Odd	Even	Odd	Even
Sgn(β)	Estimated with Eq. (4)	−	+	−	+	−	+
	Fitted with Eq. (12)	−	+	−	+	−	+

[a]Determined by the parity of the electric field patterns.

approximately at the rods. The $|\beta/2\gamma|$ estimated with the peak values of the eigenfield at the sites $q=0$ and $q=1$ is 4.64, indicating that the dispersion curves do not cross (Table I), as there is one partition row. It is worth noting that the field is confined on the line of rods along the x and y axes (assumed the single defect is located at the origin of the coordinate) to minimize the field energy. Also, the field drops rapidly apart from the axes; hence, the field decreases dramatically with q. The field at the site $q=2$ is only 1/7 of that at the site $q=1$, so the coupling with the defects $q \geqslant 2$ can be omitted without significant influence to the determination of crossing and/or anticrossing of dispersion curves. Furthermore, the field $S(d\hat{\mathbf{x}})$ at the site $q=0$ is remarkably higher than $S(d\hat{\mathbf{x}}+a\hat{\mathbf{y}})$ at the sites $q=\pm 1$, resulting in $|\beta|>|2\gamma|$. Because the field $S(d\hat{\mathbf{x}})$ is positive and the $\Delta\varepsilon(r)$ is a negative step function for air defects, β must be negative. Hence, the eigenvalue $\omega^{+}(k)$ at $k=0$ [see Eqs. (12) and (13)] has the lowest photon energy and the fundamental guided mode is odd. With the same argument as the case of one partition row, the dispersion curves with two partition rows are not crossing because the $|\beta/2\gamma|$ is estimated to be 2. However, the fundamental guided mode is of even parity because the field $S(2d\hat{\mathbf{x}})$ at the site $q=0$ is negative; thus, β is positive. We conclude that the parity of the fundamental mode is odd and/or even as there are odd and/or even rows between the PCWs in square lattices.

Alternatively, we can more accurately determine β and γ by fitting the split $\omega^{+}(k)$ and $\omega^{-}(k)$ derived by PWE (discrete data in Fig. 5). The dispersion curves are well fitted by Eq. (12) (solid curves) without taking account the coupling with defects $q \geqslant 2$, as the dispersion of a single PCW $\omega_1(k)$ is given by Eq. (7) (the dash curve). In addition, several k's in the PWE calculation are enough for fitting the coupling coefficients. The obtained ratios ($|\beta/2\gamma|$) are 5.23 and 1.3 for one and two partition rows, respectively, indicating no crossing as predicted by the estimated $|\beta/2\gamma|$. These results are verified by the electric-field patterns derived by PWE. Here, only the field patterns with one partition row are shown in Fig. 5, in which no flip of their parities occurs, indicating that the dispersion curves are not crossing and the fundamental guided mode has odd parity. Our arguments for the parity of fundamental modes (odd and/or even as the number of partition rows is odd and/or even) and no crossing of dispersion curves (see Table I) are supported by PWE.

B. Reduced-rod defects in triangular lattices

The eigenfield of a single defect in a triangular lattice appears in a higher sixfold symmetry. The parities of the fundamental mode follow the rule mentioned above, since again the peaks and valleys appear alternately at the rods similar to that in a square lattice. The difference between the eigenfields $S(d\hat{\mathbf{x}})$ at the site $q=0$ and $S(d\hat{\mathbf{x}}+a\hat{\mathbf{y}})$ at $q=\pm 1$ is rather small (see Fig. 4). Therefore, the $|\beta/2\gamma|$ estimated by peak values with one partition row is only 0.9 ($|\beta|<|2\gamma|$). With two partition rows, there is no rod for $q=0$ at the x axis, and $|\beta/2\gamma|$ is effectively much smaller than 1 (i.e., $|\beta| \ll |2\gamma|$). Hence, the $\omega^{+}(k)$ and $\omega^{-}(k)$ curves in the triangular lattice always cross, which does not occur for coupled PCWs in a square lattice with reduced-rod defects. Again, these results in terms of the parities of fundamental modes and crossing and/or anticrossing of dispersion curves in a triangular lattice are consistent with that of PWE by analyzing the field patterns of the guided modes (Fig. 6). In addition, the coupled void-rod PCWs in a triangular lattice show similar behavior (not shown here) as the reduced-rod PCWs and can also be well interpreted by the coupling of point defects.

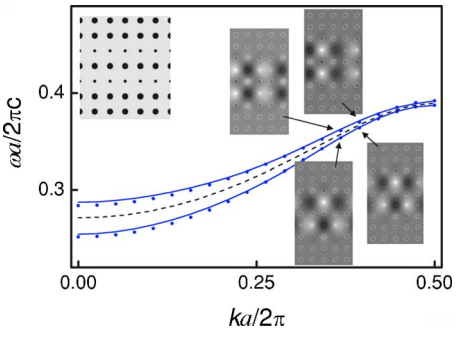

FIG. 5. (Color online) Split dispersion curves of coupled reduced-rod PCWs (inset at left top) calculated by PWE (data dots) with the electric-field guided mode patterns at the specified k's and fitted by Eq. (12) (solid curve) and the dispersion curve of one isolated PCW (dashed curve) in a square lattice.

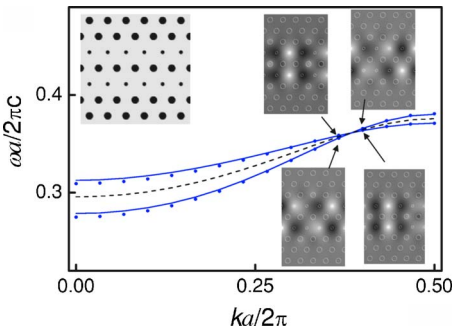

FIG. 6. (Color online) Split dispersion curves of coupled reduced-rod PCWs (inset at left top) calculated by PWE (data dots) with the electric-field guided mode patterns at the specified k's and fitted by Eq. (12) (solid curve) and the dispersion curve of one isolated PCW (dashed curve) in a triangular lattice.

C. Void-rod defects in square lattices

As the point defect is a void rod in square lattices, the eigenfield (Fig. 7) is less localized than the fields of defects in the higher-symmetry triangular lattices and of the reduced-rod defect in a square lattice. Therefore, it is unsuitable for determining $|\beta/2\gamma|$ by the peak and/or valley values. The $|\beta/2\gamma|$ values are 0.69 and 1.15 for one and two partition rows in a square lattice, respectively, derived by fitting the discrete data from PWE by Eq. (12). Hence, the $|\beta/2\gamma|$ values indicate that the $\omega^+(k)$ and $\omega^-(k)$ curves are crossing and/or anticrossing when the number of partition rows is odd and/or even, in accordance with the results in Ref. 15.

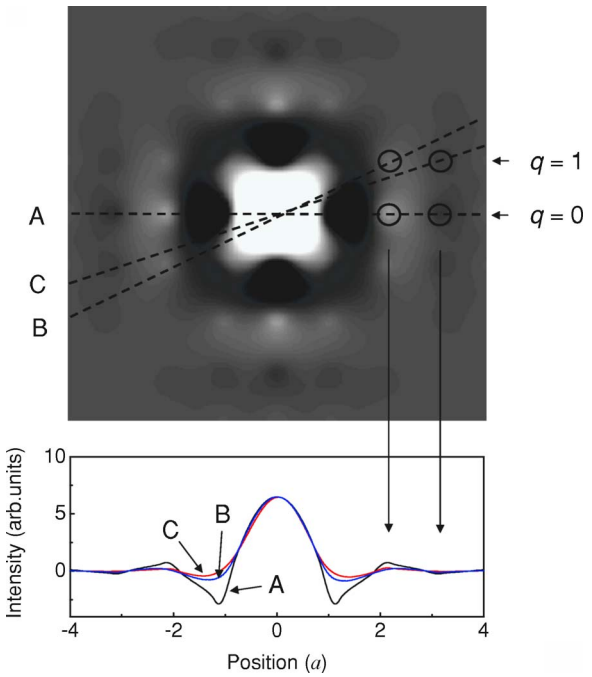

FIG. 7. (Color online) (Upper panel) The electric eigenfield pattern of a single void-rod defect in a square lattice, where circles indicate the equivalent sites of the NN ($q=0$) and next-NN defects ($q=\pm1$) when the other PCWs is separated by one and two partition rows. (Lower panel) The projected profiles (denoted as A, B, and C) passing through the various sites of neighboring defects.

Based on the theory of point-defect coupling, the parity of fundamental modes and crossing and/or anticrossing of dispersion curves can be interpreted by eigenfields of single defects. Although the cross coupling coefficients can be calculated more accurately either by using Eq. (4), which has to integrate over all the defects of the perturbed PCWs or at least those to where the eigenfield extends, or by fitting the discrete data derived by PWE, they can be estimated with the eigenfields of single defects (as long as the field distribution is not too extended). Note that the PWE calculation (e.g., the MPB program from the MIT group or commercial packages such as the "RSOFT") only gives discrete data (k's) of dispersion curves, generally, and presents "anticrossing" results even for the "crossing" cases. Whether it "anticrosses" or "crosses" is normally determined by the symmetry of the eigenfunctions before and after the "skeptical" degenerate point.

The local maxima with alternate signs (peaks and valleys) of eigenfields occur at the dielectric rods, which can be used to determine the parity of the fundamental modes. The parity is odd (even) as the number of the partition row is odd (even), whether the lattice is square or triangular, and the defect is reduced rod or void rod. In triangular lattices, because the eigenfield has a sixfold symmetry, resulting in $|\beta|<|2\gamma|$, the $\omega^+(k)$ and $\omega^-(k)$ curves are always crossing. With void-rod defects in square lattices, β and γ calculated by fitting the discrete data from PWE are more reliable for determining either crossing or anticrossing.

V. POWER TRANSFER AND COUPLING LENGTH

In this section, we derive the power transfer and coupling length, making use of the eigenmode expansion of the coupled PCWs. The wave function or field distribution in any one of the coupled PCWs on any transverse plane, e.g., at the site n, can be expressed as the superposition of the eigenfunctions of the coupled PCWs. The amplitudes in each PCW can be written as

$$\begin{pmatrix} U_n \\ V_n \end{pmatrix} = A\begin{pmatrix} U_0^+ \\ V_0^+ \end{pmatrix}\exp(ik_o na) + B\begin{pmatrix} U_0^- \\ V_0^- \end{pmatrix}\exp(ik_e na), \quad (14)$$

where U_n and V_n represent the field amplitudes in PCWs I and II, respectively, and A and B are the modal amplitudes of the eigenmodes with propagation constants k_e and k_o. Again, U_0^+, U_0^-, V_0^+, and V_0^- are obtained according to Eq. (13). The derivative of U_n with respect to the propagation distance y can be written as

$$\frac{dU}{dy} = \frac{U_{n+1} - U_n}{a} = A\exp(ik_o na)\frac{\exp(ik_o na) - 1}{a} + B\exp(ik_e na)\frac{\exp(ik_e na) - 1}{a}. \quad (15)$$

Assume that $ka \ll 1$ and $y=na$, the discrete equations [Eqs. (14) and (15)] can be rewritten as the continuous equations,

$$U(y) = A\exp(ik_o y) + B\exp(ik_e y), \quad (16)$$

$$\frac{dU(y)}{dy} = i[k_o A \exp(ik_o y) + k_e B \exp(ik_e y)]. \quad (17)$$

Similarly, $V(y)$ and its derivative can then be written as

$$V(y) = -A \exp(ik_o y) + B \exp(ik_e y), \quad (18)$$

$$\frac{dV(y)}{dy} = -i[k_o A \exp(ik_o y) + k_e B \exp(ik_e y)]. \quad (19)$$

From Eqs. (16) and (18), we can express $\exp(ik_o y)$ and $\exp(ik_e y)$ in terms of $U(y)$ and $V(y)$; therefore, the differential coupled equations [Eqs. (17) and (19)] of field functions in the individual PCWs I and II can be expressed as

$$\frac{dU(y)}{dy} = iKU(y) + iMV(y), \quad (20)$$

$$\frac{dV(y)}{dy} = iKV(y) + iMU(y), \quad (21)$$

where

$$K = \frac{k_e + k_o}{2} \text{ and } M = \frac{|k_e - k_o|}{2}, \quad (22)$$

with K and M corresponding to the effective propagation constant and the effective mutual coupling coefficient, respectively. Let $U(y)=U'(y)\exp(iKy)$ and $V(y)=V'(y)\exp(iKy)$; substituting them into Eqs. (20) and (21), we obtain the coupled mode equations of the field envelopes for the individual PCWs I and II as

$$\frac{dU'(y)}{dy} = iMV'(y) \text{ and } \frac{dV'(y)}{dy} = iMU'(y). \quad (23)$$

The solution to Eq. (23) is

$$\begin{bmatrix} U'(y) \\ V'(y) \end{bmatrix} = \begin{bmatrix} \cos(My) & i\sin(My) \\ i\sin(My) & \cos(My) \end{bmatrix} \begin{bmatrix} U'_0 \\ V'_0 \end{bmatrix}, \quad (24)$$

where $U'_0=U'(0)$ and $V'_0=V'(0)$ represent the initial conditions. It implies that complete power transfer from one PCW to the other occurs when $\cos(My)=0$; that is, $My=(m+1/2)\pi$, where m is an integer. The minimal distance of complete power transfer, i.e., the coupling length l_c, satisfies $l_c=\pi/(2M)=\pi/|k_e-k_o|$.

We have reduced the differential coupled equations [Eqs. (17) and (19)] to the coupled mode equations [Eqs. (20) and (21)] or Eq. (23), which corresponds to Eq. (1). The EM wave propagates along the coupled PCWs with an effective propagation constant equal to the average of the propagation constants of the eigenmodes of the system, and the coupling length l_c equal to $\pi/|k_e-k_o|$ is identical to that of the conventional CMT. However, the decoupling when $M=0$ is a result of cancellation among the cross couplings to the NN ($q=0$) and the next-NN ($q=\pm 1$) defects, which do not result in the loss of guiding in the individual waveguides, as occurs in the conventional coupled waveguides, which use only a single coupling coefficient C [Eq. (2)] in the CMT. Therefore, the tight-binding approximation method based on the coupling of point defects is more appropriate for deriving the coupled-mode equations and coupling length in terms of the power transfer between coupled PCWs.

VI. CONCLUSION

We introduce the concept of point-defect coupling to derive the dispersions of PCWs under the tight-binding approximation and apply it to formulate the EM wave propagation along the coupled PCWs. The dispersive behavior of coupled PCWs can be interpreted by the cross couplings due to the NN and the next-NN defects in the other PCW. The former leads to splitting of the dispersion curve of coupled PCWs. The parities of the fundamental modes are determined by the sign of its cross-coupling coefficient β and can be even or odd. The dispersion curves are further modulated by the cross coupling due to the next-NN defects. The inequality $|\beta|<|2\gamma|$ is the criterion for the crossing of the dispersions (leading to the decoupling of PCWs), which occurs at $k=[\cos^{-1}(-\beta/2\gamma)]/a$. The decoupling effect, which cannot be deduced by the conventional CMT, is a result of a balance of the cross coupling due to the NN and the next-NN defects.

The cross-coupling coefficients are strongly related to the eigenfield distribution of the single defects. Hence, the behavior of coupled PCWs with various partition rows in different lattices (i.e., square and triangular) can be interpreted by the distribution and symmetry of the eigenfields. Furthermore, the theory can obtain the coupled-mode equations and the expression for the coupling length, which is identical to the result of conventional CMT.

ACKNOWLEDGMENTS

We gratefully acknowledge partial financial support from the National Science Council (NSC) in Taiwan under Contract Nos. NSC-94-2112-M-009-035 and NSC-94-2112-M-029-004 and the Tunghai Endowment Fund for Academic Advancement.

*Authors to whom correspondence should be addressed.
†Electronic address: wfhsieh@mail.nctu.edu.tw
‡Electronic address: sccheng@faculty.pccu.edu.tw

[1] R. D. Meade, A. Devenyi, J. D. Joannopoulos, O. L. Alerhand, D. A. Smith, and K. Kash, J. Appl. Phys. **75**, 4753 (1994).
[2] A. Mekis, J. C. Chen, I. Kurland, S. Fan, P. R. Villeneuve, and J. D. Joannopoulos, Phys. Rev. Lett. **77**, 3787 (1996).
[3] M. Tokushima, H. Kosaka, A. Tomita, and H. Yamada, Appl. Phys. Lett. **76**, 952 (2000).
[4] S. Y. Lin, E. Chow, J. Bur, S. G. Johnson, and J. D. Joannopolous, Opt. Lett. **27**, 1400 (2002).
[5] K. Hosomi and T. Katsuyama, IEEE J. Quantum Electron. **38**,

825 (2002).
[6] S. Kuchinsky, V. Y. Golyatin, A. Y. Kutikov, T. P. Pearsall, and D. Nedeljkovic, IEEE J. Quantum Electron. **38**, 1349 (2002).
[7] M. Qiu, M. Mulot, M. Swillo, S. Anand, B. Jaskorzynska, A. Karlsson, M. Kamp, and A. Forchel, Appl. Phys. Lett. **83**, 5121 (2003).
[8] A. Sharkawy, S. Shi, and D. W. Prather, Opt. Express **10**, 1048 (2002).
[9] M. Koshiba, J. Lightwave Technol. **19**, 1970 (2001).
[10] F. S.-S. Chien, Y.-J. Hsu, W.-F. Hsieh, and S.-C. Cheng, Opt. Express **12**, 1119 (2004).
[11] A. Yariv, IEEE J. Quantum Electron. **9**, 919 (1973).
[12] H. Nishihara, M. Haruna, and T. Suhara, *Optical Integrated Circuits* (McGraw-Hill, New York, 1989), Chap. 3, pp. 46–52.
[13] S. Boscolo, M. Midrio, and C. G. Someda, IEEE J. Quantum Electron. **38**, 47 (2002).
[14] C. M. de Sterke, L. C. Botten, A. A. Asatryan, T. P. White, and R. C. McPhedran, Opt. Lett. **29**, 1384 (2004).
[15] T. Koponen, A. Huttunen, and P. Törmä, J. Appl. Phys. **96**, 4039 (2004).
[16] J. P. Albert, C. Jouanin, D. Cassagne, and D. Bertho, Phys. Rev. B **61**, 4381 (2000).
[17] D. N. Christodoulides and N. K. Efremidis, Opt. Lett. **27**, 568 (2002).
[18] S. G. Johnson and J. D. Joannopoulos, Opt. Express **8**, 173 (2001).
[19] A. Yariv, Y. Xu, R. K. Lee, and A. Scherer, Opt. Lett. **24**, 711 (1999).
[20] M. Bayindir, B. Temelkuran, and E. Ozbay, Phys. Rev. Lett. **84**, 2140 (2000).